ABUAD Journal of Engineering Research and Development (AJERD)
ISSN: 2645-2685

Volume 3, Issue 1, 48-58

Impact of Installation of Static Var Compensator on Available Transfer Capability on Electric Power Grid

Sunday ADETONA[1], Olatunde OGUNDEJI[2], Ayangbenjo ADEYEYE[2]

[1]*Department of Electrical & Electronics Engineering, University of Lagos, Lagos, Nigeria*
sadetona@unilag.edu.ng

[2]*Department of Electronics & Computer Engineering, Lagos State University, Epe Campus, Lagos, Nigeria*
hollabiodun@gmail.com/gbemiadeyeye@gmail.com

Corresponding Author: hollabiodun@gmail.com

Date Submitted: 04/11/2019
Date Accepted: 16/03/2020
Date Published: 30/06/2020

Abstract: *This contribution analyses the impact of installation of Static Var Compensator (SVC) on Available Transfer Capability (ATC) on Electric Power Grid (EPG). The state Bifurcation Criteria (sBC) was used to evaluate the ATC of the EPG, and also to establish optimal location for the injection of the SVC on EPG; whereas, N-1 contingency analysis (N-1CA) was utilized in identifying the most severe transmission line in the EPG. The ATCs of the grid were evaluated under normal situation and contingency with and without the injection of SVC at the identified optimal location. The Western System Coordinating Council (WSCC) 9-bus network was used as the test bed; which was modelled in PSAT in the MATLAB environment. During the simulation exercises, the ATC obtained without the injection of the SVC in the grid was 3.4380 pu to 3.6319 pu gotten with the same condition but with the injection of SVC at the identified optimal location of the same grid. When the EPG was subjected to a critical constraint, the ATC of the same grid during contingency without SVC at the optimal location was found to be 0.5372 pu; whereas with SVC injected, it was 0.6692 pu. The result reveals that ATC of the grid is significantly improved by 5.64 % when the grid is under normal conditions and when SVC is injected. The result obtained when the EPG was subjected to severe contingency also shows that the ATC of the EPG is significantly improved by 24.57 %.*

Keywords: *Available Transfer Capability, Continuation Power Flow, N-1 Contingency Analysis, Optimal location and Static Var Compensator.*

1. INTRODUCTION

Electricity markets globally are moving from well-known monopolistic regimes to deregulated or liberalized markets; where there are market participants (MPs) and operators. The MPs in the markets buy and sell electricity in deregulated markets by abiding by market rules and grid codes. The grid activities in the deregulated markets are always competitive. This is because the MPs strive to provide the best services at reduced cost; but with high volume of quality energy in their efforts to make more profits [1], and to be able to participate in the activities of the markets. Apart from the competition among MPs, the grid in the deregulated markets become opened to all MPs; and this open access and competition among MPs frequently resulting to transmission network overloading, and if not well managed, transmission networks of the grid would be congested and severely constrained. Therefore, in order to make the EPG reliable, stable, and secured, there is need to continuously evaluating ATC of the EPG from time to time. Even, in some developed economies, it is compulsory to post the information about the ATCs of EPGs on Open Access Same Time Information System (OASIS), for day-ahead and real-time reliable markets [2], [3] and [4]. Hence, the ATC of the interconnected grid and the critical transmission paths between areas (regions) must be frequently computed, updated and posted to OASIS [5]. Therefore, evaluation of ATCs, and also their enhancement remains necessary operational tool for daily routine operation in EPG [6].

Various researchers have studied evaluation and enhancement of ATCs using reliable and high-speed methods and electronic devices respectively. For instance, [7] has revealed that Optimal Power Flow (OPF) can be used for the computation of TTC, and hence for the ATC in between two different control areas of any EPG. For the purpose of maximizing ATC of the power transactions in EPG, [7] proposed the used of multi-type Flexible AC Transmission Systems (FACTS). In order to search for types, locations, and parameters of multi-type FACTS that would maximize power transactions in EPG, [7] also suggested the usage of Improved Evolutionary Programming (IEP). The test results on the various test beds used indicated that optimally placed OPF with FACTS by IEP enhanced TTC value far more than OPF without FACTS.

Knowing fully well that to obtain the suitable solutions using OPF method require convexity of objective function [8]; therefore [9], in their work then used Continuation Power Flow (CPF) to compute ATCs for a set of source and sink transfers. In order to find optimal location for the static SVC, they used Genetic Algorithm (GA). Also, [10] used CPF in computation of ATC of EPG, but used Real-Code GA; an improved version of the GA, to find the best location for the injection and size setting of both SVC and Thyristor Controlled Series Compensator (TCSC) so as to enhance ATC. Both [10], and [9] used Saddle Node Bifurcation (SNB) limit of the CPF; which uses only steady state stability limit to determine loading parameter which is essential parameter in determining ATC of a given EPG.

It has been established by [11] that in convectional CPF, the same loading factor is used for a particular constellate of generators and loads; and as such, a conservative ATC value may be obtained, therefore, instead of using CPFs, the DC load flow Power Transfer Distribution Factor (DCPTDF) for quick assessment of ATC was proposed by [12]. The work of [12] though computed ATCs of the EPG very fast, but results obtained were erroneous. These errors are due to some assumptions made in formulation of the DC load flow; for instance, considerations of nominal voltage at all buses of the grid, disusing of charging capacitance of the lines, and believing that line losses are negligible. Just because of the weaknesses of the DCPTDF, [13] therefore proposed the utilization of AC load flow Power Transfer Distribution Factor (ACPTDF) in a combined economic emission dispatch (CEED) environment for computation of ATC values of EPG; but used Weight Improved Particle Swarm Optimization (WIPSO) algorithm to obtain optimal settings and location of SVC in an EPG so as to increase its ATC values.

The above literature review and many more on ATC determination reveal that most of the work considered only the static limits as the system constraints. To that effect, [14] therefore proposed the usage of State Bifurcation Criteria (sBC) for the computation of ATC of EPG. The sBC takes care of both static and dynamic limits as the system constraints. In the work of [14], Voltage State Participation Factor (VSPF) was employed in placing SVC in optimal location for the purpose of enhancing ATC of the EPG. For ATC to be enhanced, [14] suggested that SVC should be placed at a load bus that has maximum VSPF. As good as the work of [14], it failed to examine effects SVC on ATC when EPG is under different forms of contingencies. Also, Saddle node and Hopf bifurcation limits used in [14] for the evaluation of maximum loading condition for the purpose of computation of grid's static and dynamic ATCs only made use of steady state stability and small signal stability limits respectively. As a result of these shortcomings, this study therefore makes use other type of BC that is better than the one used in [14] to determine impact of SVC on EPG when it is under normal and contingency situations.

2. METHODOLOGY

2.1 Determination of ATC

ATC is the transfer capability left over in the physical transmission network for supplementary commercial action over and above previously committed uses. Mathematically [4], [5], [15]:

$$ATC = TTC - TRM - ETC - CBM \tag{1}$$

In equation (1);

TTC = Total Transfer Capability; and is defined as the volume of electric energy that can be relocated over power grid network in a reliable manner while meeting all of a specific set of defined pre and post contingency conditions [10].

TRM = Transmission Reliability Margin; and is the quantity of transfer capability necessary to provide a reasonable level of assurance that the power grid system will be secure.

CBM = Capacity Benefit Margin; is the amount of transfer capability preserved for Load Service Entities (LSE's) on the host transmission system where their load is located, to enable an access to generation from the grid systems and to meet generation reliability requirements.

ETC = Existing Transmission Commitments; and is the volume of power which has been already committed or scheduled, that is, the base case load on the system [16].

It has been established in [14], [16] and [17] that TRM and CBM are adjudicated by germane policies of the system operator and the MPs; consequently, equation (1) becomes

$$ATC = TTC - ETC \tag{2}$$

The ETC in equation (2) is a Base Case Power (BCP) solution [16] [17]; which is defined as the sum of active loads on some buses of interest of an EPG. These active loads are obtained when EPG is subjected to load flow analysis. Therefore, if P_{Loi} denotes the active load on bus i, then the BCP is

$$BCP = ETC = \sum_{i=1}^{NB} P_{Loi} \tag{3}$$

In equation (3) NB = total number of buses in a given EPG that connects an area (region) to another area (region). The TTC in equation (2) can be expressed as

$$TTC = BCP + \lambda \ BCP = (1 + \lambda)BCP \quad (4)$$

In equation (4) λ represents the loading parameter that varies the base case of generator power P_{GO}, reactive power Q_{Lo} and load P_{LO}. Upon using equation (4) in equation (2), we obtained

$$ATC = \lambda BCP = \lambda \sum_{i=1}^{NB} P_{Loi} \quad = \lambda_C \sum_{i=1}^{NB} P_{Loi} \quad (5)$$

Equation (5) reveals that ATC is a function of critical loading parameter and Base Case Power; that is, $ATC = f(\lambda_C, BCP)$. In (5) λ_C is maximum power loading margin (critical loading parameter); which can be defined as the system $loadability$ at base case and at different contingencies.

2.1.1 Evaluation of λ_C and $|V|_{weakest}$ using sBC

In this study, sBC is employed to find λ_C, and consequently ATC on the EPG; and also to establish suitable location for the injection of SVC under four different conditions. Bifurcation conjecture addresses an abrupt change in the system behaviour as certain system parameter (λ) is increased. In this study, we are interested in determination of critical loading parameter λ_C ; which can be obtained in the sBC by Saddle-Node Bifurcation (SNB) point, or Hopf Bifurcation limit (HBL), or a CPF technique [18]. In the CPF analysis, generator $MVars$ limit, or voltage limit or flow limit of transmission network of an EPG is used in identifying λ_C ; whereas, in evaluating λ_C for the purpose of computing ATC, SNB and HBL only make use of steady state stability point and small signal stability limit respectively. This shows that CPF approach makes use of any of the three limits that occurs first to establish λ_C in a given EPG; whereas SNB and HBL each has only one limit. This shows that CPF approach is far better than SNB and HBL, and hence used in this study.

The CPF problem of an EPG according to [18] can be explained as the solution of a nonlinear set of equations:

$$\dot{x} = f(x, y, \lambda) = 0 \quad (6)$$

$$0 = g(x, y, \lambda) \quad (7)$$

Equations (6) and (7) are differential and algebraic equations (DAE) respectively. In these equations, x and y are the dynamic state and algebraic variables respectively. The λ in these equations represents the loading parameter that varies the base case of generator power P_{GO}, load P_{LO} and reactive power Q_{LO}, as follows

$$P_G = (\lambda + \gamma k_G)P_{Go} \quad (8)$$

$$[P_L, Q_L] = \lambda \ [P_{Lo}, Q_{Lo}] \quad (9)$$

In equations (8) and (9), γ and k_G are the generator participation coefficients and distributed slack bus variable respectively.

Figure 1 shows that the CPF uses prediction and correction steps to find successive load flow solutions based on a varying load parameter λ at different time.

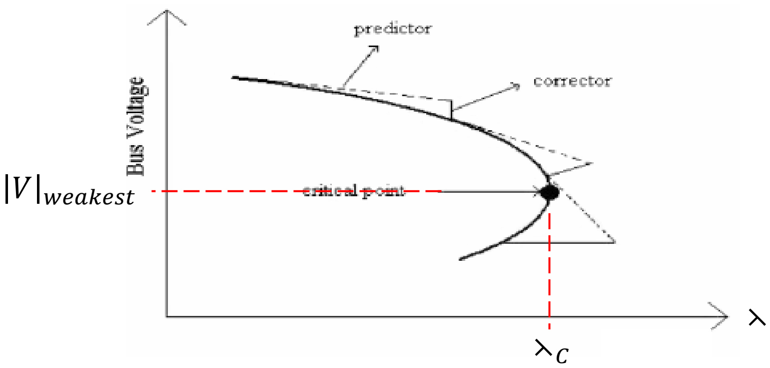

Figure 1: The P-V curve illustrating the prediction-correction step of CPF [19]

For a specified pattern of load increase, a tangent predictor uses a known BCP solution to estimate next solution. Newton Raphson Load Flow (NRLF) algorithm is employed and the corrector step is determined. After that, a new prediction is made for a specified increase in load based upon the new tangent vector, and then corrector step is applied. The weaker buses in an EPG are identified by the dimension of tangent vector from the CPF solution. The worst (weakest) bus is the one which is experiencing voltage collapse and on the P-V curves, it is the one that is contiguous to the nose of the curve [19].

The algebraic variables y depend upon the loading parameter λ. At the initial operating point, $\dot{x} = 0,\ x = x_0\ , and\ y = y_0$. If there are incremental changes in variables over the initial values, then DAE, that is, equations (6) and (7) become

$$\Delta\dot{x} = \frac{\partial f}{\partial x}\Big|_{x_0, y_0} \Delta x + \frac{\partial f}{\partial y}\Big|_{x_0, y_0} \Delta y + \frac{\partial f}{\partial \lambda}\Big|_{x_0, y_0} \Delta \lambda \quad (10)$$

$$0 = \frac{\partial g}{\partial x}\Big|_{x_0, y_0} \Delta x + \frac{\partial g}{\partial y}\Big|_{x_0, y_0} \Delta y + \frac{\partial g}{\partial \lambda}\Big|_{x_0, y_0} \Delta \lambda \quad (11)$$

In equations (6) and (7), $\frac{\partial f}{\partial \lambda}\Big|_{x_0, y_0} \Delta \lambda = \frac{\partial g}{\partial \lambda}\Big|_{x_0, y_0} \Delta \lambda = 0$; this is because λ is a constant parameter. Hence equations (10) and (11) become

$$\Delta\dot{x} = \frac{\partial f}{\partial x}\Big|_{x_0, y_0} \Delta x + \frac{\partial f}{\partial y}\Big|_{x_0, y_0} \Delta y = A\Delta x + B\Delta y \quad (12)$$

$$0 = \frac{\partial g}{\partial x}\Big|_{x_0, y_0} \Delta x + \frac{\partial g}{\partial y}\Big|_{x_0, y_0} \Delta y = C\Delta x + D\Delta y \quad (13)$$

In equations (12) and (13), $A, B, C, and\ D$ are elements of the Jacobian matrix; and from equation (13), it is evident that

$$\Delta y = -CD^{-1}\Delta x \quad (14)$$

Upon using equation (14) in equation (12), we obtained

$$\Delta\dot{x} = [A - BCD^{-1}]\Delta x = \overset{\frown}{A}\,\Delta x \quad (15)$$

The $\overset{\frown}{A} = [A - BCD^{-1}]$ in equation (15) is referred to as a reduced Jacobian matrix of the EPG.

$$\Delta x = [A - BCD^{-1}]^{-1}\Delta\dot{x} = \left[\overset{\frown}{A}\right]^{-1} \Delta\dot{x} \quad (16)$$

The reduced Jacobian matrix of an EPG modifies NRLF algorithm greatly. The non-convergence of the modified NRLF algorithm due to the generator $MVars$ limit or voltage limit or flow limit of transmission network of the EPG determines $\lambda_C\ and\ |x|_{weakest} = |V|_{weakest}$. The λ_C obtained via equation (16) gives ATC from one area of the grid to another area of the same grid as given in equation (5) and invariably equation (2); whereas, $|V|_{weakest}\ at\ bus\ i$ gives the bus where SVC must be injected for the ATC to be enhanced.

2.1.2 N-1 Contingency Analysis

Congestion often occurs in the EPG due to line outage, generator outage, change in energy demand and uncoordinated transactions. In this study, N-1 contingency analysis (N-1CA) is used to ascertain the most critical line outage in an EPG. This is because it allows computing MW flow limits in transmission lines and transformers by considering transmission line thermal, generator $MVars$ and voltage security limits; and voltage stability constraints [20].

In N-1CA, a CPF analysis (which was discussed in subsection 2.1.1 of this paper) is carried out for each line outage of the EPG. During the analysis, if the $\lambda_C < 1$, the outage line is ignored; and donned to be an infeasible line. On completion of the analysis, all the contingencies are sequentially arranged in a "$worst\ line\ contingency$" order; with aim of obtaining the minimum power flows $(MWs)_{min}$ in each transmission networks. These $(MWs)_{min}$ are the power flow limits, and output of the N-1CA.

2.2 Dynamic Model and Sizing of SVC

2.2.1 Dynamic Model of SVC

The dynamic model of SVC [21] adopted in this study is presented in Figure 2. In the figure, V_{ref} = Reference voltage; and V_i = feedback voltage from $bus\ i$ where SVC is injected; K_R = The regulator gain; τ_d = Time constant as a result of the time lag in injecting of firing pulses; τ_b = Firing circuit time constant and τ_R = Regulator time constant. Also, from the figure, it is evident that $B_{Lmax} \leq B_{ref} \leq B_{Cmax}$.

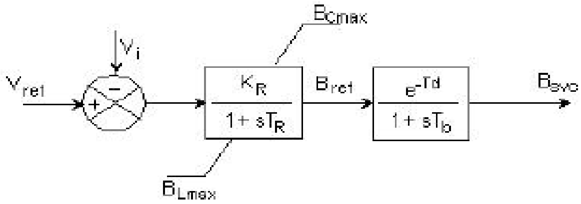

Figure 2. The dynamic model SVC

It is evident from Figure 2 that the model is an open loop system; and its transfer function $G(s)$ is

$$G(s) = \frac{B_{SVC}(s)}{V_{ref}(s) - V_i(s)} = \frac{K_R e^{-s\tau_d}}{(1 + s\tau_R)(1 + s\tau_b)} \tag{17}$$

Therefore,

$$B_{SVC}(s) = \frac{K_R e^{-s\tau_d}}{(1 + s\tau_R)(1 + s\tau_b)} \left(V_{ref}(s) - V_i(s)\right) \tag{18}$$

And for the steady-state analysis, equation (18) becomes

$$B_{SVC}(s)|_{s\to 0} = \frac{K_R e^{-s\tau_d}}{(1 + s\tau_R)(1 + s\tau_b)} \left(V_{ref}(s) - V_i(s)\right)\Big|_{s\to 0} = K_R \left(V_{ref}(s) - V_i(s)\right) \tag{19}$$

Equation (19) can be expressed in $t-domain$ as

$$B_{SVC} = K_R\left(V_{ref} - V_i\right) \tag{20}$$

And it is well known from the electric circuit theory that reactive power Q_m injected at $bus\ m$ can be expressed as

$$Q_m = V_m^2 B_{mm} = V_m^2 B_{SVC} = V_m^2\, K_R\left(V_{ref} - V_m\right) = K_R\left(V_m^2 V_{ref} - V_m^3\right) \tag{21}$$

Whereas, the general expression for the reactive power Q_m at $bus\ m$ using load flow analysis is

$$Q_m = -|V_m| \sum_{k=1}^{n} |Y_{mk}|\,|V_k| sin(\theta_{mk} - \delta_m + \delta_k) \tag{22}$$

If SVC is injected in $bus\ m$, Q_m has to be modified to Q_m^c anytime $|V_m|$ is not within 0.95 $|V_m| \leq |V_m| \leq 1.05\ |V_m|$. The expression for Q_m^c at $bus\ m$ using load flow analysis now becomes

$$Q_m^c = -|V_m| \sum_{k=1}^{n} |Y_{mk}|\,|V_k| sin(\theta_{mk} - \delta_m + \delta_k) - K_R\left(V_m^2 V_{ref} - V_m^3\right) \tag{23}$$

It should be stated here that when SVC is installed in $bus\ m$, the elements of Jacobian matrix for the computation of state variables in NRFL domain, will also change. If it is assumed that the Jacobian element affected by injecting $SVC\ at\ bus\ m\ \ is\ J_{mm}$; then

$$J(m, m) = J_{mm} \equiv \frac{\partial Q_m^c}{\partial |V_m|} = -\sum_{k=1}^{n} |Y_{mk}|\,|V_k| cos(\theta_{mk} - \delta_m + \delta_k) - 2K_R|V_m|\left(V_{ref} - \frac{3|V_m|^2}{2}\right) \tag{24}$$

Equation (24) brings about enhancement in ATC of the EPG.

2.2.2 Sizing of SVC

Equations (17) and (18) reveal that for the dynamic sizing of SVC, $K_R, \tau_d, \tau_R, \tau_b, and\ V_{ref}$ have to be specified; whereas for the steady state sizing of SVC, $K_R and\ V_{ref}$ are only needed to be provided. It has been revealed in [21] that K_R ranges from 20 pu (5% slope) to 100 pu (1% $slope$) on the SVC base, τ_R ranges from 20 $ms\ to$ 150 ms, and τ_b is of the order of 3 $ms\ to$ 6 ms; whereas, 0.95 $pu\ \leq |V_{ref}| \leq 1.05\ pu$.

2.3 Modelling and Simulation of the Test Bed

The test bed used to investigate the effects of SVC on ATC during normal and contingency situations is Western System Coordinating Council (WSCC) 9 bus system. The test bed has 3 generators and 3 load buses. The swing bus is bus 1, whereas buses 2 and 3 are generators' buses; while buses 5, 7 and 9 are load buses. The generators capacity, the loads data and the lines parameters of the test bed are available in [22]. The maximum and minimum acceptable voltage magnitudes at all load buses are taken as 1.05 pu and 0.95 pu; whereas, the base MVA used in the test bed is set at 100 MVA.

The test bed was modelled in Power System Analysis Toolbox (PSAT 2.1.3) package. The package is based on MATLAB; and it was developed by [20]. The one line diagram of the test bed under normal situation but without the injection of SVC in PSAT environment in MATLAB is presented in Figure 3; while Figure 4 shows the PSAT model of the same bed with the outage of the most severed line; but without injection of SVC. Figures 5 and 6 show the PSAT model of the test bed when SVC is installed in optimal location under normal and critical constrained respectively.

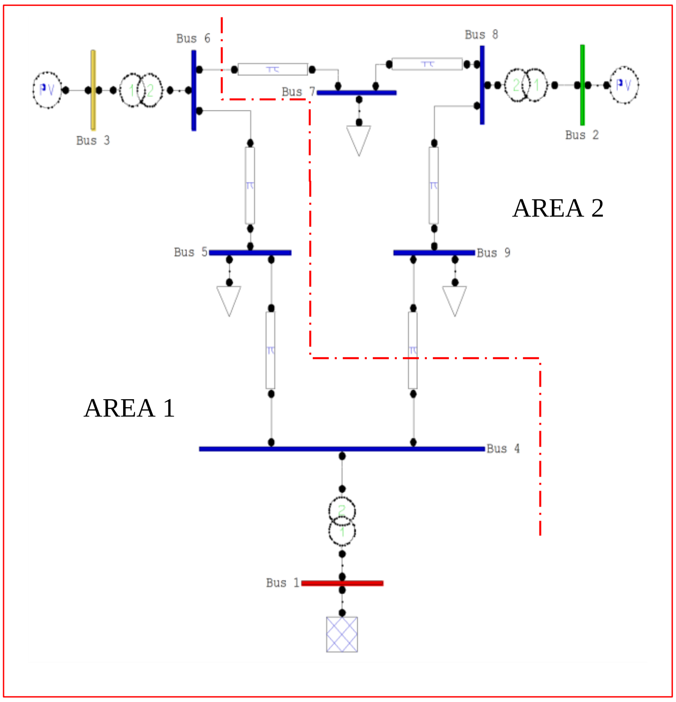

Figure 3
The PSAT model of the Test Bed under normal situation without injection of SVC

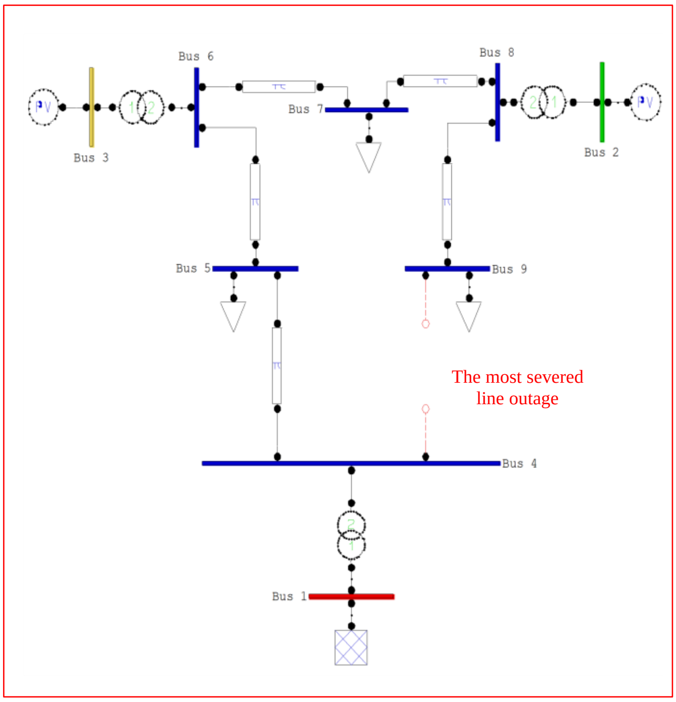

Figure 4
The PSAT model of the Test Bed with the outage of the most severed line and without injection of SVC

The test bed is divided into two different areas; area 1 and area 2, as shown in Figure 3; in order to compute its ATCs under four different situations. Buses 1, 3, 4, 5, and 6 belong to area 1; while, buses 2, 7, 8, and 9 are in area 2. The tie-lines between the two areas are therefore $Line$ 4 – 9, and $Line$ 6 – 7.

The load flow of the test bed when the system was not constrained as presented in Figure 3 was run in the PSAT in the MATLAB environment, so as to obtain BCP (ETC) values has revealed in equations (2) and (3).

To identify the most severed line of the test bed to be outage, so as to cause severe overloading (SOL) in the other parts of the bed; Figure 3 was subjected to N-1CA in the PSAT in MATLAB environment. The results obtained are discussed in section 4 of this paper; and the outage of a line that connects bus 4 to bus 9 is depicted in Figure 4.

In order to identify the optimal location for the injection of the SVC on the test bed, and to determine critical loading parameter (TTC) of each of the buses of the test bed at normal and contingency situations, Figures 3 and 4 are subjected to the CPF in the PSAT in MATLAB environment respectively. The results obtained for the TTC are discussed in section 4; and the one obtained in relation to the optimal location of the SVC dictated the position of the SVCs in Figures 5 and 6.

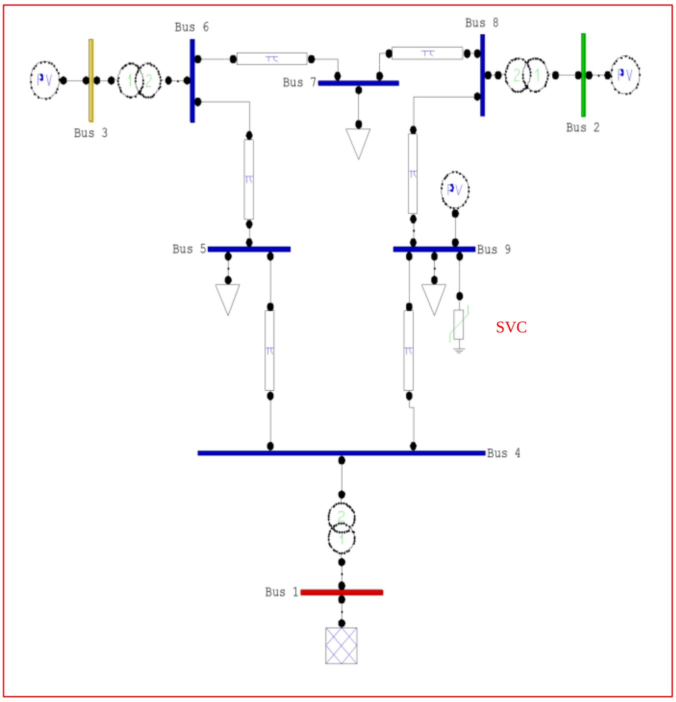

Figure 5
The PSAT model of the Test Bed under normal situation with the injection of SVC

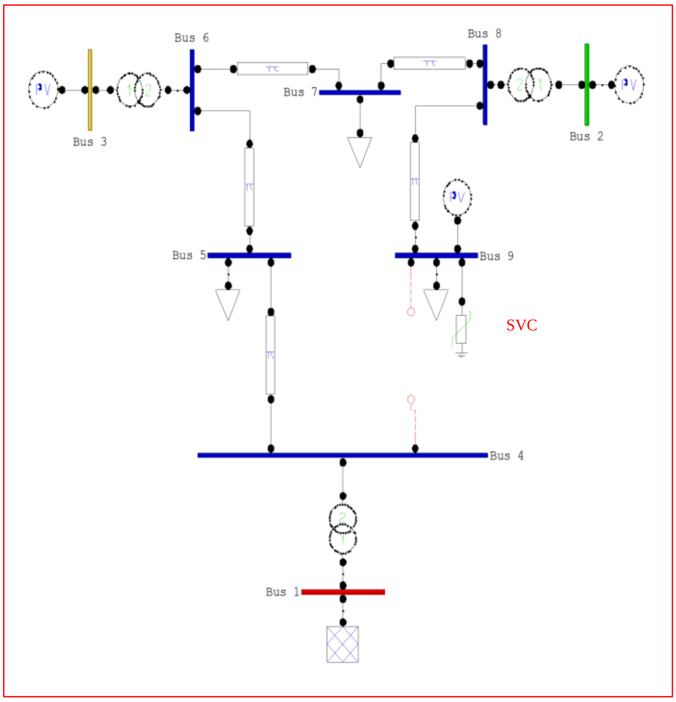

Figure 6
The PSAT model of the Test Bed with the outage of the most severed line and with the injection of SVC

3. RESULTS AND DISCUSSION

3.1 Determination of ATC of the Test bed without and with SVC

3.1.1 Determination of ATC of the Test bed under normal situation without SVC

The results obtained in the PSAT in the MATLAB environment when load flow of the test bed was run when the system was not constrained and SVC was not installed are presented in Table 1. Table 1 reveals that the voltage magnitudes of all the buses of the test bed at the base case, when it was not critically constrained and SVC was not injected, were within allowable voltage limits. The two buses that connect area 2 to area 1 are buses 7 and 9; and the connections are through tie lines 6-7 and 4–9; therefore, upon using equation (3) and data from Table 1, we obtained the ETC component of ATC viz:

$$BCP = ETC = \sum_{i=1}^{2} P_{Loi} = P_{Lo7} + P_{Lo9} = 1.0000 + 1.5000 = 2.2500\ pu$$

The TTC component of ATC was obtained from the results obtained upon subjecting Figure 3 to the CPF analysis in the PSAT in MATLAB environment. The results obtained are presented in Table 2 and Figure 7.

Table 1: The load flow results of the Test Bed under normal situation without injection of SVC

Bus	V pu	Phase rad	P_{Gen} pu	Q_{Gen} pu	P_{load} pu	Q_{load} pu
1	1.0400	0.0000	0.7164	0.2686	0.0000	0.0000
2	1.0250	0.1558	1.6300	0.0564	0.0000	0.0000
3	1.0250	0.0845	0.8500	-0.1048	0.0000	0.0000
4	1.0259	-0.0387	0.0000	0.0000	0.0000	0.0000
5	1.0129	-0.0644	0.0000	0.0000	0.9000	0.3000
6	1.0327	0.0343	0.0000	0.0000	0.0000	0.0000
7	1.0162	0.0126	0.0000	0.0000	1.0000	0.3500
8	1.0260	0.0649	0.0000	0.0000	0.0000	0.0000
9	0.9958	-0.0696	0.0000	0.0000	1.2500	0.5000

Table 2: The CPF results of the Test Bed under normal situation without injection of SVC

Bus	V pu	Phase rad	P_{Gen} pu	Q_{Gen} pu	P_{load} pu	Q_{load} pu
1	1.0400	0.0000	2.1821	2.9132	0.0000	0.0000
2	1.0250	0.4751	4.1206	2.7455	0.0000	0.0000
3	1.0250	0.2302	2.1488	1.5242	0.0000	0.0000
4	0.8869	-0.1367	0.0000	0.0000	0.0000	0.0000
5	0.8067	-0.2326	0.0000	0.0000	2.2752	0.7584
6	0.9412	0.0905	0.0000	0.0000	0.0000	0.0000
7	0.8557	0.0278	0.0000	0.0000	2.5280	0.8848
8	0.8994	0.2101	0.0000	0.0000	0.0000	0.0000
9	0.7182	-0.2865	0.0000	0.0000	3.1600	1.2640

Table 2 shows that five different buses were not within allowable voltage limits; whereas Figure 7 reveals that the worst bus is bus 9. Based on Table 2, the TTC component of the ATC is computed as following:

$$TTC = \sum_{i=1}^{2} P_{Li} = P_{L7} + P_{L9} = 2.5280 + 3.1600 = 5.6880\, pu\,;$$

Therefore, upon using the values of the BCP and TTC in equation (2), we obtained

$$ATC = TTC - ETC = 5.6880 - 2.2500 = 3.4380\, pu$$

This shows that the ATC of the test bed under normal situation without injection of SVC was 3.4380 pu .

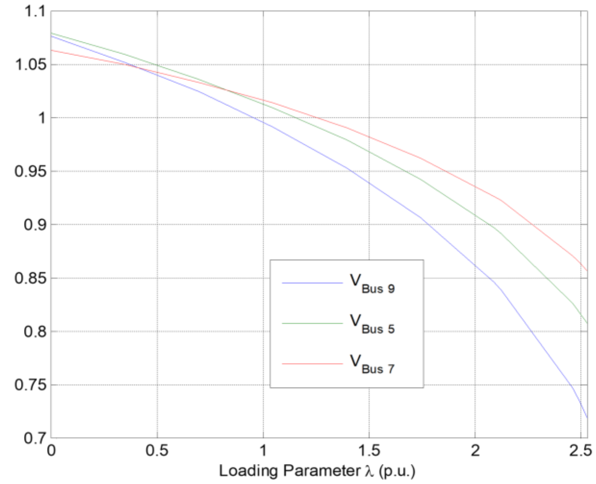

Figure 7: The plot of λ-V when the Bed is not constrained and SVC not injected

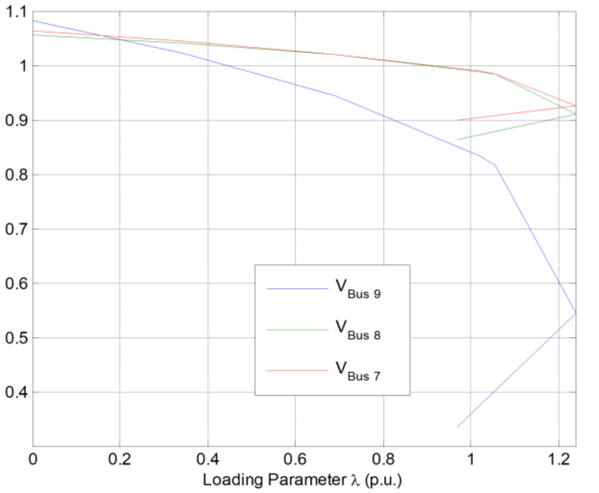

Figure 8: The plot of λ-V when the Bed was constrained but SVC was not injected in an optimal location

3.1.2 Determination of ATC of the Test Bed under severe contingency without SVC in an optimal location

The results obtained in the PSAT in the MATLAB environment when the test bed was subjected to the N-1CA, to identify the mostly severed transmission line in the grid, in order to evaluate the ATC of the grid under severe contingency with and without the injection of SVC at an optimal location, are presented in Table 3. The results obtained reveal that the tie line 9-4 is the mostly severed transmission line; and hence removed from the test bed. The resulting test bed with most severed line outage is presented in Figure 4.

Table 3: The results obtained when the Test Bed was subjected to N-1CA

Line	Outage of this line	Worst Case	$P_{ij(Base)}$ pu	$P_{ij(max)}$ pu	$S_{ij(Base)}$ pu	$S_{ij(max)}$ pu
7-6	Feasible	9-4	0.2418	0.9771	0.3426	1.1241
7-8	Feasible	6-5	0.7638	0.2193	0.7665	0.2240
5-4	Unfeasible	7-6	0.3070	0.3031	0.3468	0.4901
9-4	Feasible	6-5	0.4094	0.1840	0.5610	0.5353
8-9	Feasible	7-8	0.8662	0.0004	0.8702	0.1430
6-5	Feasible	9-4	0.6082	0.0847	0.6343	0.1765
3-6	Unfeasible	7-6	0.8500	0.8654	0.8629	1.1524
2-8	Unfeasible	9-4	1.6300	2.0711	1.6326	2.7452
1-4	Unfeasible	9-4	0.7164	1.0165	0.7651	1.0257

Table 4: The CPF results of the Test Bed under severe contingency without injection of SVC

Bus	V pu	Phase rad	P_{Gen} pu	Q_{Gen} pu	P_{load} pu	Q_{load} pu
1	1.0400	0.0000	1.1659	0.2108	0.0000	0.0000
2	1.0250	-0.1346	2.0192	2.1377	0.0000	0.0000
3	1.0250	-0.1049	1.0529	0.4694	0.0000	0.0000
4	1.0304	-0.0627	0.0000	0.0000	0.0000	0.0000
5	0.9966	-0.1637	0.0000	0.0000	1.1149	0.3716
6	0.9985	-0.1693	0.0000	0.0000	0.0000	0.0000
7	0.9250	-0.2791	0.0000	0.0000	1.2388	0.4336
8	0.9101	-0.2618	0.0000	0.0000	0.0000	0.0000
9	0.5433	-0.7458	0.0000	0.0000	1.5484	0.6194

The TTC component of ATC was obtained from the results obtained upon subjecting Figure 4 to the CPF analysis in the PSAT in MATLAB environment. The results obtained are presented in Table 4 and Figure 9. Table 4 shows that only one bus is not within allowable voltage limits; whereas Figure 10 reveals that the worst bus is bus 9; and hence the bus to be injected SVC. The parameters of the SVC employed in this contribution for the purpose of enhancing ATC are: Power rating = $100\ MVA$, Voltage rating = $230\ kV$, Frequency = $50\ Hz$, Reference voltage = $1.00\ pu$, Capacitive reactance $X_c = 0.10\ pu$, Inductive reactance $X_l = 0.20\ pu$, $B_{max} = 1.00\ pu$, $B_{min} = -1.00\ pu$, K_R = Regulator gain = $100\ pu$, and τ_d = Time constant as a result of the time lag in injecting of firing pulses = $25\ ms$.

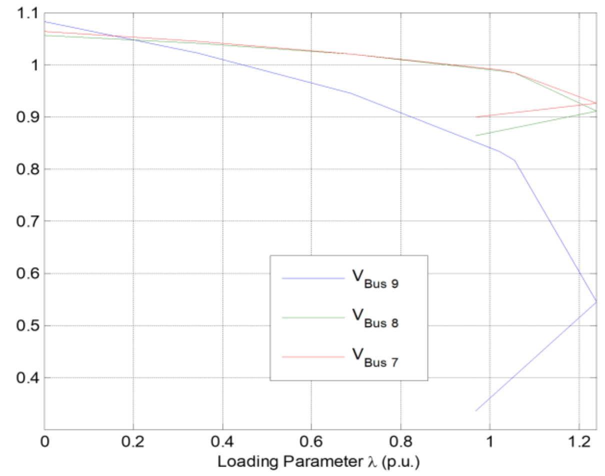

Figure 9: The plot of λ-V plot when the Bed was not constrained but SVC was injected in an optimal location

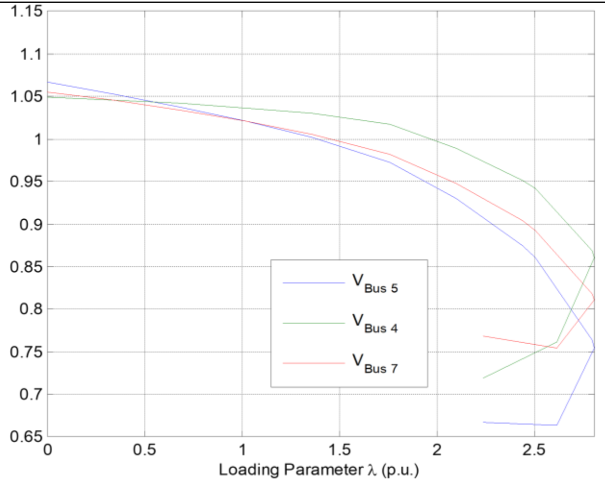

Figure 10: The plot of λ-V when the Bed was constrained and SVC was injected in an optimal location

Based on Table 4, the TTC component of the ATC is computed as following:

$$TTC = \sum_{i=1}^{2} P_{Li} = P_{L7} + P_{L9} = 1.2388 + 1.5484 = 2.7872\ pu$$

Therefore, upon using the values of the BCP and TTC in equation (2), we obtained

$$ATC = TTC - ETC = 2.7872 - 2.2500 = 0.5372\ pu$$

This shows that the ATC of the test bed under severe contingency without the injection of SVC was $0.5372\ pu$

3.1.3 Determination of ATC of the Test Bed under normal situation with SVC installed in optimal location

The results obtained in the PSAT in the MATLAB environment when the test bed was subjected to the CPF when the system was not constrained but SVC was installed in an optimal location are presented in Table 5 and Figure 9.

Table 5: The CPF results of the Test Bed under normal situation with the injection of SVC in an optimal location

Bus	V pu	Phase rad	P_{Gen} pu	Q_{Gen} pu	P_{load} pu	Q_{load} pu
1	1.0400	0.0000	2.7034	5.3083	0.0000	0.0000
2	1.0250	0.5943	4.2611	4.6329	0.0000	0.0000
3	1.0250	0.2478	2.2220	2.5581	0.0000	0.0000
4	0.7609	-0.1981	0.0000	0.0000	0.0000	0.0000
5	0.6636	-0.3404	0.0000	0.0000	2.3527	0.3716
6	0.8795	0.0932	0.0000	0.0000	0.0000	0.0000
7	0.7539	0.0299	0.0000	0.0000	2.6142	0.7843
8	0.7982	0.2842	0.0000	0.0000	0.0000	0.0000
9	0.4526	-0.5681	0.0000	0.0000	3.2677	1.1022

Table 6: The CPF results of the Test Bed under severe contingency with the injection of SVC in an optimal location

Bus	V pu	Phase rad	P_{Gen} pu	Q_{Gen} pu	P_{load} pu	Q_{load} pu
1	1.0400	0.0000	0.9875	0.1178	0.0000	0.0000
2	1.0250	-0.0496	2.1148	0.1390	0.0000	0.0000
3	1.0250	-0.0423	1.1028	-0.0060	0.0000	0.0000
4	1.0349	-0.0529	0.0000	0.0000	0.0000	0.0000
5	1.0090	-0.1375	0.0000	0.0000	1.1677	0.3892
6	1.0276	-0.1077	0.0000	0.0000	0.0000	0.0000
7	1.0060	-0.1944	0.0000	0.0000	1.2974	0.4541
8	1.0242	-0.1680	0.0000	0.0000	0.0000	0.0000
9	1.0216	-0.4373	0.0000	0.0000	1.6218	-0.3802

Table 5 reveals that the voltage magnitudes of all the buses of the test bed at the base case, when it was not critically constrained and SVC was not injected, were within allowable voltage limits. Based on Table 5, the TTC component of the ATC is computed as following:

$$TTC = \sum_{i=1}^{2} P_{Li} = P_{L7} + P_{L9} = 2.6142 + 3.2677 = 5.8819\, pu$$

Therefore, upon using the values of the BCP and TTC in equation (2), we obtained

$$ATC = TTC - ETC = 5.8819 - 2.2500 = 3.6319\, pu$$

This shows that the ATC of the Test Bed under normal situation with SVC installed in optimal location of the bed was 3.6319 pu

3.1.4 Determination of ATC of the Test Bed under severe contingency with SVC in an optimal location

The results obtained in the PSAT in the MATLAB environment when the test bed was subjected to the CPF when the system was constrained and SVC was installed in an optimal location so as to compute the test bed's TTC are presented in Table 6 and Figure 10. Table 6 reveals that the voltage magnitudes of all the buses of the test bed at the base case, when it was critically constrained and SVC was injected in an optimal location, were within allowable voltage limits Based on Table 6, the TTC component of the ATC is computed as following:

$$TTC = \sum_{i=1}^{2} P_{Li} = P_{L7} + P_{L9} = 1.2974 + 1.6218 = 2.9192\, pu$$

Therefore, upon using the values of the BCP and TTC in equation (2), we obtained

$$ATC = TTC - ETC = 2.9192 - 2.2500 = 0.6692\, pu$$

This shows that the ATC of the Test Bed under severe contingency with SVC in an optimal location of the bed was 0.6692 pu

3.2 Discussion

The value of ATC of the test bed under normal condition without the injection of SVC at the optimal location method is found to be 3.4380 pu; whereas, the value of ATC of the same grid during a severe contingency without installation of SVC at any location of the test bed is found to be 0.5372 pu; and this represents about 84.38 % reduction in the values of the ATC. These results reveal that $ATCs$ of the $EPGs$ under severe contingencies are normally reduced drastically; and as such, there should be concerted efforts to minimize outages of most severed lines in any EPG. The results also show that the value of ATC of the test bed under normal condition with the injection of SVC at optimal location increases from 3.4380 pu to 3.6319 pu; and this typifies about 5.64 % increase in the values of the ATC. These results indicate that $ATCs$ of $EPGs$ under normal conditions can be enhanced significantly with an injection of SVC at optimal location.

From the simulation results, it is also evident that the ATC of the test best under contingency but with the injection of SVC at optimal location is 0.6692 pu, whereas its value under the same situation but without installation of SVC at any location is 0.5372 pu; and this represents about 24.57 % increase in the values of the ATC. The difference in the values of the ATC during normal condition, and contingency with and without SVC is an indication that SVC or any other relevant $FACT$ become necessary to be included on the grids not only to enhance their ATC values; but also to increase the efficiency of operation of the existing networks, without building new lines.

4. CONCLUSION

This contribution has shown that $ATCs$ of an EPG under normal condition and a severe contingency are enhanced significantly with an installation of SVC at an optimal location of the EPG; therefore, the stakeholders in the liberalized or deregulated electricity markets especially in the developing economies should embrace the injections of $SVCs$ and other relevant $FACTs$ at the suitable locations of their $EPGs$. It is also revealed in this study that when an EPG is under a severe contingency, its ATC reduces drastically either the EPG in question has SVC injected at optimal location or not; therefore, there should be concerted efforts on the part of system operators (SOs) in the liberalized or deregulated electricity markets to make sure that outages of most severed lines on their $EPGs$ are adequately minimized, and effectively controlled.

This study only investigates the impact of the installation of SVC on EPG with the aim of enhancing the $ATCs$ of the EPG in question. The installation of the device may be okay technologically; what of its economic implications and realization? To that effect, there is need to examine the economic implications of injecting SVC at an optimal location of an EPG with the aim of enhancing its $ATCs$.

ACKNOWLEDGMENT

The authors are pleased to acknowledge the support provided by the Department of Electronics and Computer Engineering (ECE), Lagos State University, Epe Campus, Lagos, Nigeria.

REFERENCES

[1] Omorogiuwa, E., & Harrison E., (2018). Determination of Available Transfer Capacity (ATC) in a Competitive Electricity Market Using Nigerian 3-bus and 14-bus power network as Case Study. Nigerian Journal of Technology, 37(3):786 -794.
[2] Federal Energy Regulatory Commission (FERC), (1999). Regional Transmission Organizations. Washington, DC, (1999). Docket RM99-2-000, order 2000.
[3] Ravinder, K., & Ashwani K., (2015). Impact of STATCOM Control Parameters on Available Transfer Capability Enhancement in Energy Markets" 4th International Conference on Eco-friendly Computing and Communication Systems, (ICECCS), Procedia Computer Science, 70 (2015): 515 – 525.
[4] North American Electric Reliability Council, (1996). Available Transfer Capability Definitions and Determination: A framework for determining Available Transfer Capabilities of the interconnected transmission networks for a commercially viable electricity market. NJ, 1-42.
[5] Nireekshana T., Kesava R.G., & Siva N.R.S., (2012). Enhancement of ATC with FACTS devices Using Real-code Genetic Algorithm, Electrical Power and Energy Systems, 43(2012):1276–1284.
[6] Seong L.C., (2007). Analysis of Available Transfer Capability (ATC) of Transmission System Using MATLAB" BSc Report, University Malaysia Perlis (UniMAP).
[7] Ongsakul, W., & Jirapong, P., (2009). Optimal Placement of Multi-Type FACTS Devices to Enhance Total Transfer Capability using Improved Evolutionary Programming, International Journal of Energy Technology and Policy, 7(2): 180-200.
[8] Lai, L.L. (1998) Intelligent System Applications in Power Engineering: Evolutionary Programming and Neural Networks, Singapore, John Wiley and Sons
[9] Sandhya R. B., & Suresh R., (2013). Enhancement of ATC by Optimal Allocation of TCSC and SVC by Using Genetic Algorithm, IOSR Journal of Electrical and Electronics Engineering, 7(3): 24-31
[10] Sabitha K.., & Bhasha S.J., (2014). Enhancement of ATC with Facts Devices using Real-Code Genetic Algorithm, International Journal of Engineering Research & Technology, 3(8): 1005-1012
[11] Gravener, M.H., & Nwankpa, C., (1999). Available transfer capability and first order sensitivity, IEEE Transactions on Power Systems, 14(2): 512–518.
[12] Christie R.D., Wollenberg B.F., & Wangensteen I., (2000). Transmission Management in the Deregulated Environment, Proceedings of the IEEE, 88(2): 170-195.
[13] Sripriya R. & Neela, R. (2016). SVC Placement for ATC Enhancement using WIPSO Technique, Global Journal of Pure and Applied Mathematics, 12(1): 747-760.
[14] Sanjay K.C, Srivastava S.C., & Kumar A., (2002). Available Transfer Capability Determination using Bifurcation Criteria and its Enhancement through SVC Placement, National Power Systems Conference, NPSC 2002, Indian Institute Of Technology, Kharagpur, 721302, 721-726.
[15] Feng W., & Shrestha G.B., (2001). Allocation of TCSC devices to Optimize Total Transmission Capacity in a Competitive Power Market, IEEE Transactions on Power Systems: 5, (2001): 87–92.
[16] Sadiq A.A., Adamu S.S., & Buhari M., (2019). Available transfer capability enhancement with FACTS using hybrid PI-PSO, Turkish Journal of Electrical Engineering and Computer Sciences, 27(4):2881-2897.
[17] Adetona S.O., Salawu R.I., & Okafor F.N., (2014). Simulink model for planning a new power transmission investment, Simulation, 90(2): 171–181.
[18] Canizares, C. A., (2002). Voltage Stability Assessment: Concepts, Practices and Tools, Technical report, IEEE/PES Power System Stability Subcommittee, Final Document. Available at http://www.power.uwaterloo.ca
[19] Kishore, A., and Hill, E.F., (1971). Static Optimization of Reactive Power Sources by use of Sensitivity Parameters, IEEE Trans on Power Apparatus and Systems, 90(1971): 1166-1173.
[20] Milano F., (2005). An open source power system analysis toolbox. IEEE Transactions on Power Systems; 20(2005): 1199–1206.
[21] Srivastava K.N. (1994). Investigations into Static and Dynamic Aspects of Voltage Stability, PhD Dissertation, IIT Kanpur.
[22] UW, EE, University of Washington, College of Engineering. Power systems test case archive, http://www.ee.washington.edu/research/pstca/pf9/ieee9cdf.txt (accessed 26 August 2006).